Electronic supporting information

Slow magnetic relaxation in a lanthanide helix chain compound $[Dy(HNA)(NA)_2(NO_3)]_n$

Shuang Liu[a], Lei-Lei Li[b], Han Li[b], Hong-Ling Gao[a], Jian-Zhong Cui*[a] and Peng Cheng*[b]

[a] *Department of Chemistry, Tianjin University, Tianjin, 300072, China.*
[b] *Department of Chemistry, Key Laboratory of Advanced Energy Material Chemistry, MOE, and Collaborative Innovation Center of Chemical Science and Engineering (Tianjin), Nankai University, Tianjin 300071, China.*

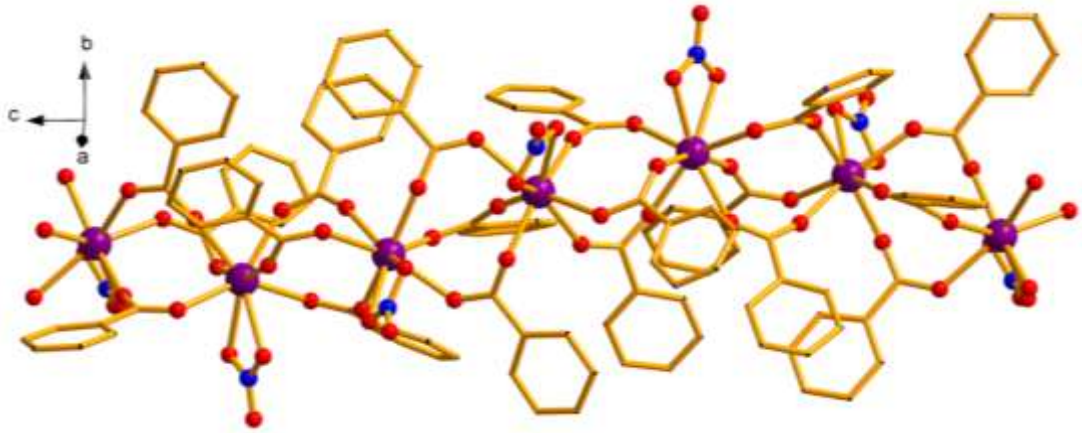

Fig. S1 1D chain structure observed in compound **1**.

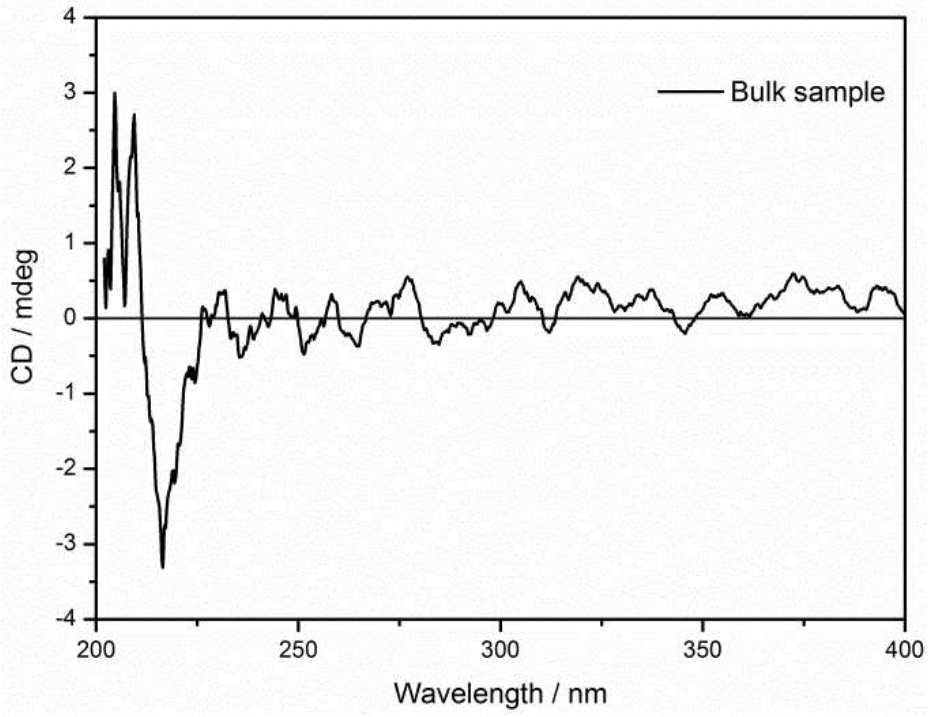

Fig. S2 Solid-state CD spectrum of **1** in bulk sample.

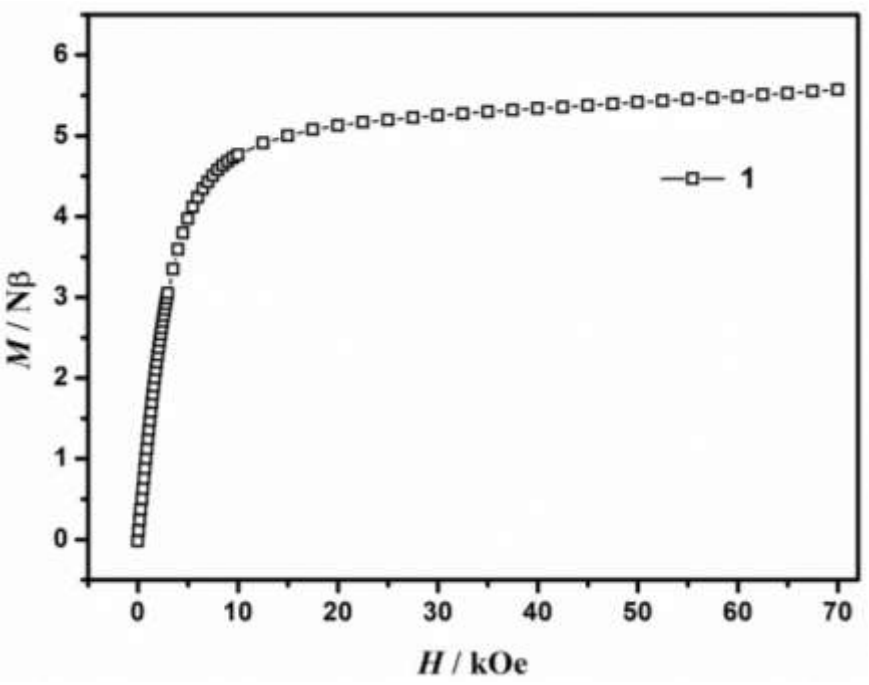

Fig. S3 Magnetization versus field of **1** at 2 K.

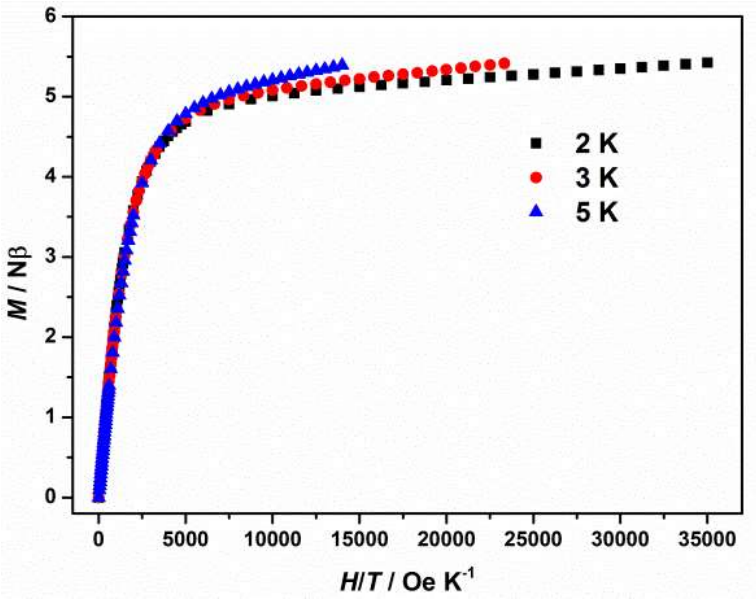

Fig. S4 Field dependence of the magnetization at different temperatures of **1**.

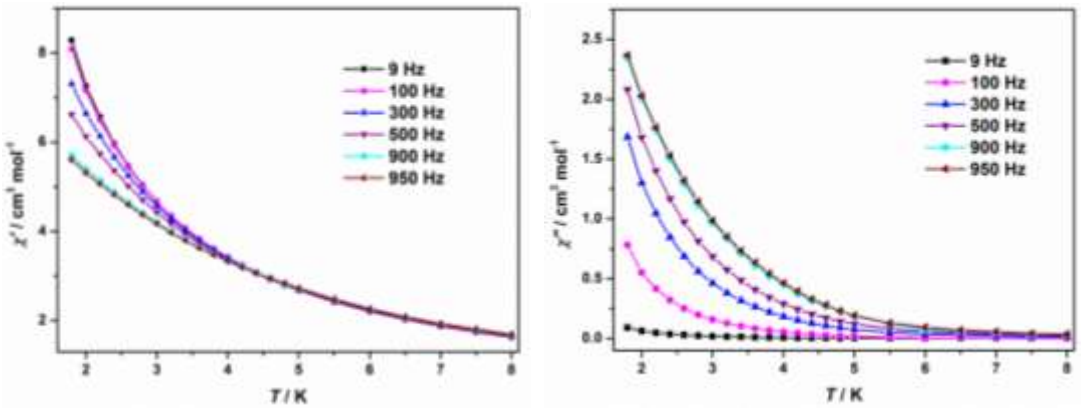

Fig. S5 Temperature dependence of in-phase and out-of-phase ac susceptibility component at different frequencies for **1** with zero dc field and an oscillation of 2.5 Oe.

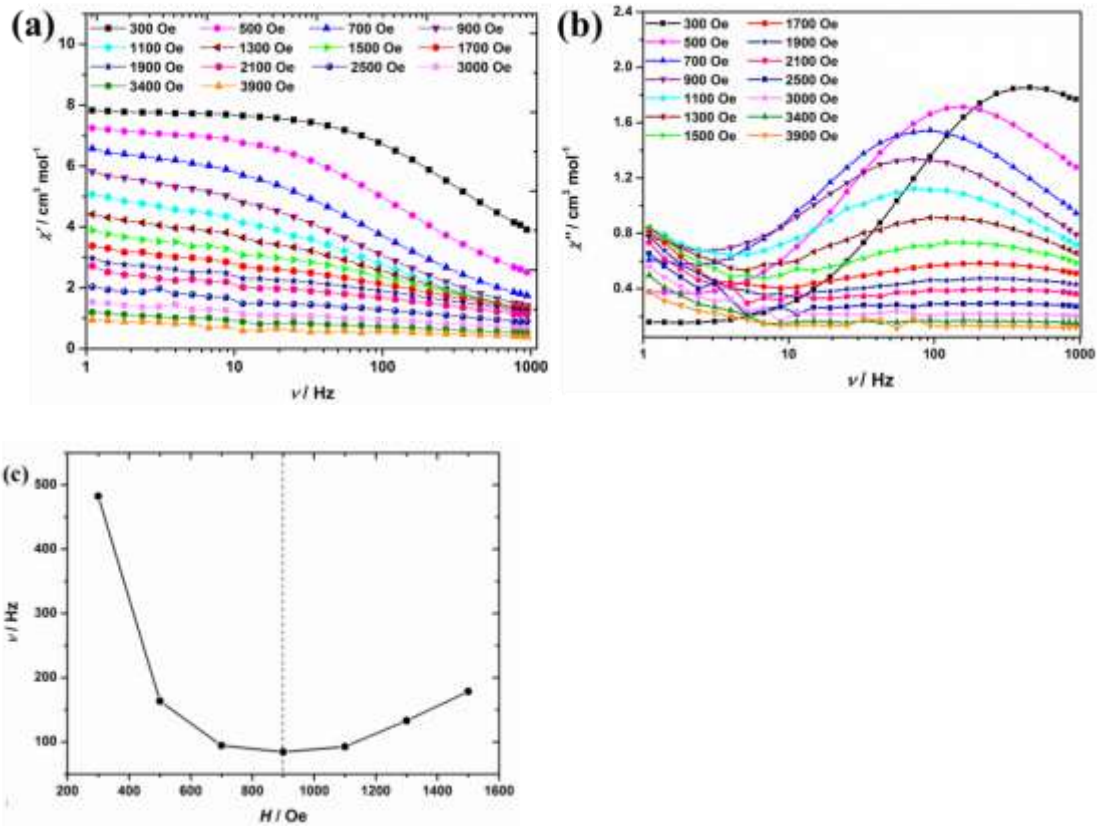

Fig. S6 Frequency dependence of the in-phase (a) and out-of-phase (χ'') (b) ac susceptibility components for **1** measured at 1.8 K with different dc fields and an oscillation of 2.5 Oe; (c) Field dependence of the frequency from χ'' vs ν data.

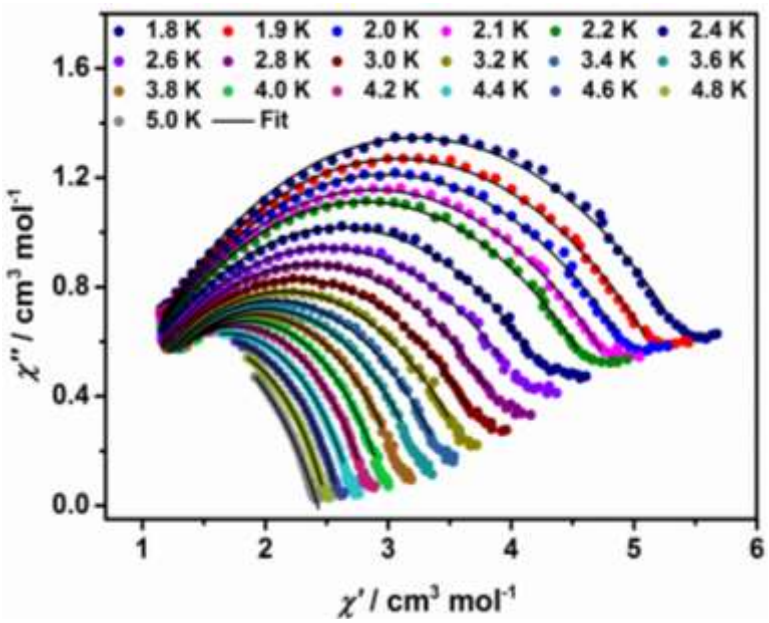

Fig. S7 Cole-Cole diagram for **1** at indicated temperatures under 900 Oe dc fields. The black lines are fitting results by Debye model.

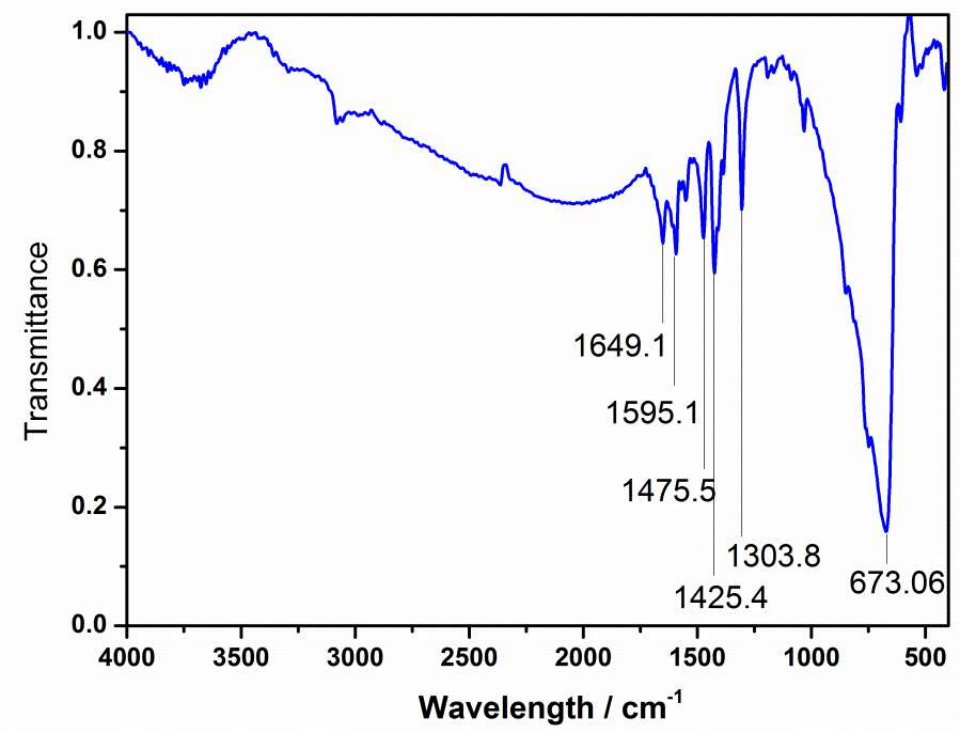

Fig. S8 The IR spectrum of compound **1**.

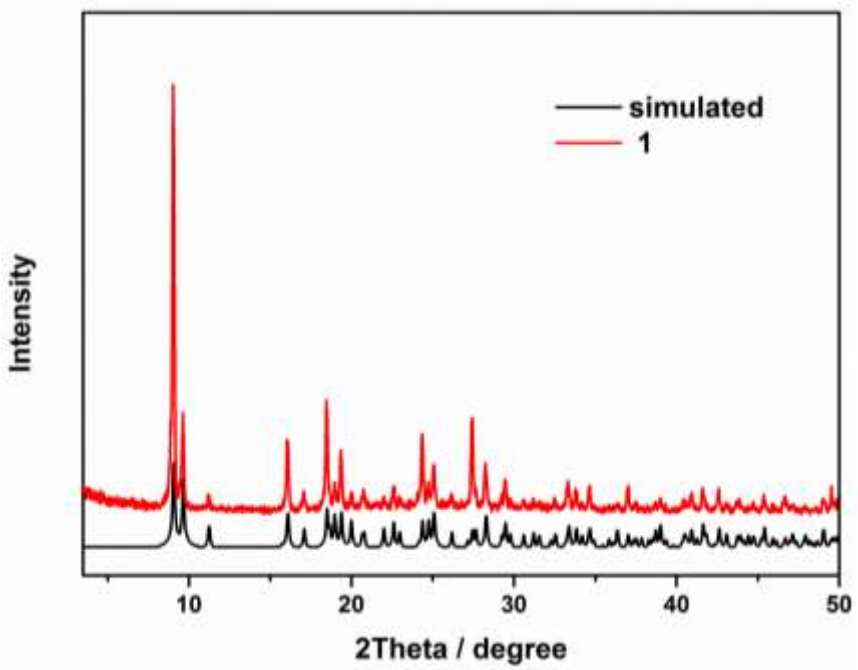

Fig. S9 Comparison of experimental and simulated powder XRD patterns of **1**.

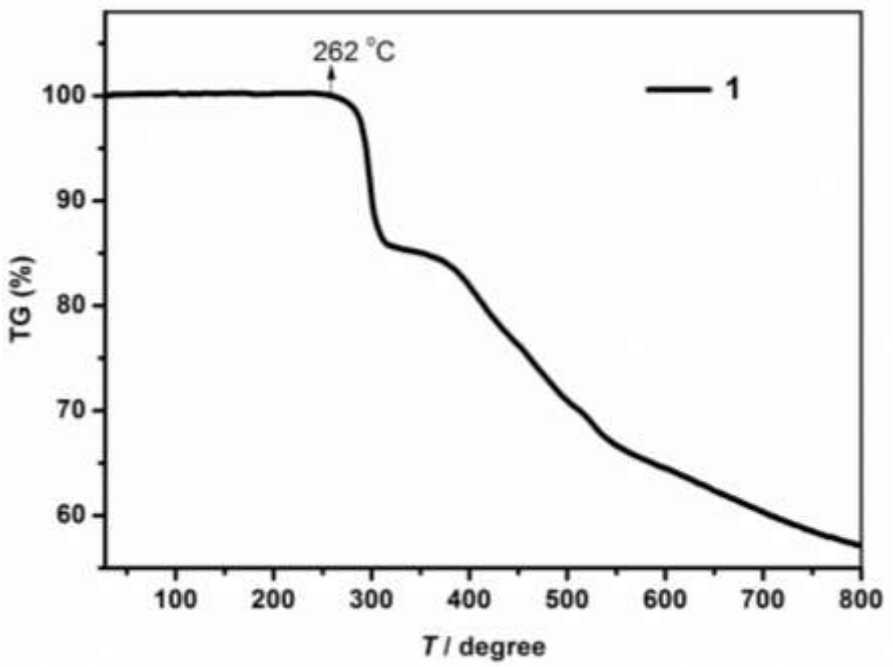

Fig. S10 There is no weight loss from room temperature to about 260 °C, corresponding to no free guest molecules in the compound. As the temperature continues to rise, dramatic weight loss occurs because of the decomposition of the organic ligands.

Table S1 Data collection and refinement for compounds **1-*P*6$_1$** and **1-*P*6$_5$**.

Compound	**1**–*P*6$_1$	**1**–*P*6$_5$
CCDC no.	1008253	1008252
formula	$C_{18}H_{13}DyN_4O_9$	$C_{18}H_{13}DyN_4O_9$
M	591.82	591.82
Temperature (K)	128(2)	128(2)
crystal system	hexagonal	hexagonal
space group	*P*6$_1$	*P*6$_5$
a / Å	11.2159(8)	11.1993(9)
b / Å	11.2159(8)	11.1993(9)
c / Å	26.5973(18)	26.5836(18)
α / deg.	90	90
β / deg.	90	90
γ / deg.	120	120
V / Å^3	2897.6(3)	2887.5(4)
Z	6	6
D_c/g cm^{-3}	2.035	2.042
μ/mm^{-1}	3.931	3.945
F(000)	1722	1722
R(int)	0.0511	0.0492
total reflections	5641	5649
Unique reflections	2249	2241
R_1[a] [I>2σ(I)]	0.0338	0.0282
wR_2[b][I>2σ(I)]	0.0740	0.0530
GOF	1.041	1.028
Flack	-0.027(18)	-0.019(15)

Table S2 Selected bond lengths (Å) and angles for compounds **1-*P*6$_1$** and **1-*P*6$_5$**.

1-*P*6$_1$		**1-*P*6$_5$**	
Bonds/Angles (Å / °)		Bonds/Angles (Å / °)	
Dy(1)-O(6)#1	2.252(7)	Dy(1)-O(5)	2.262(6)
Dy(1)-O(2)#2	2.310(7)	Dy(1)-O(4)#1	2.303(6)
Dy(1)-O(1)	2.393(7)	Dy(1)-O(6)#1	2.395(6)
Dy(1)-O(7)	2.458(7)	Dy(1)-O(7)	2.458(6)
Dy(1)-O(4)#2	2.295(7)	Dy(1)-O(1)	2.285(6)
Dy(1)-O(3)	2.350(7)	Dy(1)-O(2)#2	2.344(6)
Dy(1)-O(5)	2.397(7)	Dy(1)-O(3)	2.398(6)
Dy(1)-O(8)	2.481(7)	Dy(1)-O(8)	2.483(6)
Dy(1)-O(4)#2	2.295(7)	Dy(1)-O(1)	2.285(6)
O(6)#1-Dy(1)-O(4)#2	160.1(2)	O(5)-Dy(1)-O(1)	160.1(2)
O(6)#1-Dy(1)-O(2)#2	83.0(3)	O(5)-Dy(1)-O(4)#1	83.3(2)
O(4)#2-Dy(1)-O(2)#2	82.2(2)	O(1)-Dy(1)-O(4)#1	81.9(2)
O(6)#1-Dy(1)-O(3)	100.0(3)	O(5)-Dy(1)-O(2)#2	99.6(2)
O(4)#2-Dy(1)-O(3)	84.3(3)	O(1)-Dy(1)-O(2)#2	84.8(2)
O(2)#2-Dy(1)-O(3)	143.8(3)	O(4)#1-Dy(1)-O(2)#2	143.7(2)
O(6)#1-Dy(1)-O(1)	83.6(3)	O(5)-Dy(1)-O(6)#1	83.5(2)
O(4)#2-Dy(1)-O(1)	79.0(2)	O(1)-Dy(1)-O(6)#1	104.8(2)
O(2)#2-Dy(1)-O(1)	71.3(2)	O(4)#1-Dy(1)-O(6)#1	73.6(2)
O(3)-Dy(1)-O(1)	73.2(2)	O(2)#2-Dy(1)-O(6)#1	142.68(19)
O(6)#1-Dy(1)-O(5)	83.6(2)	O(5)-Dy(1)-O(3)	84.0(2)
O(4)#2-Dy(1)-O(5)	104.8(2)	O(1)-Dy(1)-O(3)	78.7(2)
O(2)#2-Dy(1)-O(5)	73.5(2)	O(4)#1-Dy(1)-O(3)	71.41(17)
O(3)-Dy(1)-O(5)	142.7(2)	O(2)#2-Dy(1)-O(3)	72.94(19)
O(1)-Dy(1)-O(5)	143.6(2)	O(6)#1-Dy(1)-O(3)	143.9(2)
O(6)#1-Dy(1)-O(7)	127.2(2)	O(5)-Dy(1)-O(7)	126.9(2)
O(4)#2-Dy(1)-O(7)	72.7(2)	O(1)-Dy(1)-O(7)	73.0(2)
O(2)#2-Dy(1)-O(7)	132.9(2)	O(4)#1-Dy(1)-O(7)	132.80(19)
O(3)-Dy(1)-O(7)	73.2(2)	O(2)#2-Dy(1)-O(7)	73.49(19)
O(1)-Dy(1)-O(7)	137.7(2)	O(6)#1-Dy(1)-O(7)	75.13(19)
O(5)-Dy(1)-O(7)	75.3(2)	O(3)-Dy(1)-O(7)	137.5(2)
O(6)#1-Dy(1)-O(8)	75.7(2)	O(5)-Dy(1)-O(8)	75.5(2)
O(4)#2-Dy(1)-O(8)	123.9(2)	O(1)-Dy(1)-O(8)	124.2(2)
O(2)#2-Dy(1)-O(8)	140.6(2)	O(4)#1-Dy(1)-O(8)	140.9(2)
O(3)-Dy(1)-O(8)	73.4(2)	O(2)#2-Dy(1)-O(8)	73.17(19)
O(1)-Dy(1)-O(8)	136.6(2)	O(6)#1-Dy(1)-O(8)	71.71(19)
O(5)-Dy(1)-O(8)	71.6(2)	O(3)-Dy(1)-O(8)	136.40(19)
O(7)-Dy(1)-O(8)	51.9(2)	O(7)-Dy(1)-O(8)	51.80(17)

Symmetry codes: For **1-*P*6$_1$**, #1 x-y+1,x,z+1/6; #2 y,-x+y+1,z-1/6; For **1-*P*6$_5$**, #1 x-y,x-1,z-1/6; #2 y+1,-x+y+1,z+1/6.

Table S3 The continuous symmetry measurement value calculated by *SHAPE* 2.0 for **1**.

Dy^{3+}	D_{2d} TDD	C_{2v} BTPR	D_{4d} SAPR
1-p61	1.876	2.014	2.521
1-p65	1.874	2.022	2.546

Table S4 The parameters obtained from Cole-Cole plots of **1** using the Debye model.

T / K	χ_1	χ_2	α_1
1.8	0.42	6.02	0.43
1.9	0.44	5.74	0.43
2.0	0.42	5.55	0.44
2.1	0.44	5.34	0.44
2.2	0.44	5.17	0.44
2.4	0.45	4.79	0.44
2.6	0.44	4.55	0.45
2.8	0.46	4.28	0.45
3.0	0.48	4.03	0.44
3.2	0.48	3.86	0.45
3.4	0.56	3.58	0.41
3.6	0.64	3.37	0.38
3.8	0.66	3.19	0.36
4.0	0.71	3.01	0.32
4.2	0.67	2.86	0.31
4.4	0.65	2.73	0.31
4.6	0.62	2.61	0.30
4.8	0.57	2.50	0.31
5.0	0.38	2.41	0.32